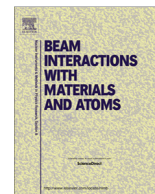


Contents lists available at [ScienceDirect](http://ScienceDirect.com)

Nuclear Instruments and Methods in Physics Research B

journal homepage: www.elsevier.com/locate/nimb

Luminescence properties of $\text{La}_2\text{O}_3:\text{Eu}^{3+}$ nanophosphor prepared by sol–gel method

N. Pushpa^{a,b}, M.K. Kokila^{a,*}, N.J. Shivaramu^c^a Department of Physics, Bangalore University, Bangalore 560 056, India^b Department of Physics (S & H), PES University, Bangalore 560 085, India^c Indian Academy Degree College, Bangalore 560 043, India

ARTICLE INFO

Article history:

Received 12 November 2015

Received in revised form 8 April 2016

Accepted 12 April 2016

Available online 19 April 2016

Keywords:

X-ray diffraction

Gamma rays

Thermoluminescence

ABSTRACT

Undoped and Eu^{3+} doped La_2O_3 nanophosphor are synthesized by low temperature sol–gel technique. The synthesized samples are characterized by X-ray diffraction (XRD) and average crystallite size is found to be ~ 18 nm and ~ 23 nm for undoped and Eu^{3+} doped La_2O_3 respectively. Gamma ray irradiated undoped La_2O_3 shows high intense thermoluminescence (TL) glow peak at 640 K and weak TL glow peak at 443 K and the high intense peak intensity is sub linear increase with γ -dose. Whereas Eu^{3+} doped La_2O_3 nanophosphor show a prominent TL glow peak at 640 K and its TL intensity linearly increases up to 1 kGy. The kinetic parameters are estimated using glow curve deconvoluted (GCD) technique. TL emission of γ -ray irradiated Eu^{3+} doped La_2O_3 show peaks at 508, 586, 619 and 706 nm are attributed to Eu^{3+} transition peaks.

© 2016 Elsevier B.V. All rights reserved.

1. Introduction

Rare earth sesquioxides have been extensively studied in recent years due to their unique electronic, optical, and chemical properties [1–3]. Among these oxides lanthanum oxide (La_2O_3) has a number of industrial and technological applications [4,5]. Sesquioxides can be obtained in the form of thin films, nanoparticles and single crystals, have been investigated for their potential applications in luminescent displays, dosimetry, and light emitting diodes (LEDs). Further Ln^{3+} ions can easily substitute in La^{3+} lattice due to similar chemical, ionic radii and electro negativity of La^{3+} ion and resulting in high efficient optical, electrical and magnetic properties. Due to quantum confinement effect, optical and luminescent properties more efficient in nano size than bulk materials.

Thermoluminescence (TL) is observed when a material irradiated for gamma, X-ray, beta and heavy ion beams etc, part of the irradiation energy is used to transfer electrons to traps. This energy, stored in the form of the trapped electrons, is released by raising the temperature of the material, and the released energy is converted to luminescence. Material such as $\text{LiF}:\text{Mg}$, $\text{CaSO}_4:\text{Dy}$, $\text{CaF}_2:\text{Dy}$ and $\text{Al}_2\text{O}_3:\text{C}$ are good thermoluminescence materials because of their applications in radiation dose measurement, age determination and defect structure analysis in solids [6,7].

However, these materials not suitable for high dose measurement because TL intensity saturates at lower doses due to the overlapping of ionized zones [8]. Hence, research has been going on to improve the dosimetry applications of nano materials by changing synthesis technique or adding inorganic and organic agents [9,10].

A wide variety of techniques are available for preparation of nano materials such a solid state reaction, sol gel, microwave synthesis, ball milling, hydrothermal, solution combustion and co-precipitation methods [9]. Among these techniques sol–gel technique is adopted for the synthesis of La_2O_3 nano particles because, this technique yields products of a high surface area to volume ratio, high homogeneity and allows fine control of the chemical composition [10,11]. In the present work, gamma ray irradiated TL glow curve and TL emission properties of undoped and Eu^{3+} doped La_2O_3 nanoparticles are studied.

2. Materials and methods

Undoped and Europium doped lanthanum oxide nano materials are synthesized by sol–gel technique using lanthanum oxide [99.8% pure (La_2O_3), Aldrich chemicals], anhydrous citric acid [99.5% pure GR ($\text{C}_6\text{H}_8\text{O}_7$), Merck chemicals], Europium oxide [99.9% pure (Eu_2O_3), Aldrich chemicals] and nitric acid [(HNO_3) , Merck chemicals] as raw materials. The ratio of citric acid to La^{3+} is considered as 2.0 [10]. Stoichiometric amount of lanthanum oxide and europium oxide are separately dissolved with dilute

* Corresponding author.

E-mail address: drmkokila@gmail.com (M.K. Kokila).

nitric acid to get lanthanum nitrate and europium nitrate followed by dissolving in 50 ml of double distilled water. The resultant solutions are mixed and refluxed at room temperature for 3 h. Finally, the stoichiometric amount of citric acid is slowly added, to act as a chelating agent and refluxed at 60–65 °C for 3 h. During refluxing, the solution slowly evaporated and turned into a reddish brown gel. Then gel is dried at 110 °C in an oven to obtain powder and annealed at 800 °C for 4 h.

The Phase purity of the samples is characterized by X-ray diffraction (XRD) technique using Rigaku Miniflex II diffractometer with Cu K α ($\lambda = 1.541 \text{ \AA}$) radiation. For TL measurements, 30 mg of nanophosphor is exposed to γ -rays (^{60}Co) in a dose range 0.05–12.00 kGy. TL measurements are carried out using TL Reader (model: TL1009I; Nucleonix Systems Pvt Ltd, India) in the temperature range 325–750 K. TL emission recorded using Ocean Optics spectrometer (USB4000).

3. Results and discussions

3.1. X-ray diffraction

Fig. 1 shows the XRD patterns of annealed undoped and Eu^{3+} doped La_2O_3 . All the diffraction peaks are well indexed as a hexagonal phase with space group P3m-1 (JCPDS card No. 05-0602) and the lattice parameter are found to be $a = 4.036 \text{ \AA}$, $c = 6.201 \text{ \AA}$ and $a = 3.397 \text{ \AA}$, $c = 6.129 \text{ \AA}$ for undoped and doped La_2O_3 respectively [12]. It is observed that weak diffraction peaks at 36.07°, 46.95° and 56.25° are indexed to $\text{La}(\text{OH})_3$. Presence of hydroxide peaks in the sample due to the hygroscopic nature of La_2O_3 at room temperature. The average crystallite size is calculated by Scherrer's formula and found to be $\sim 18 \text{ nm}$ and $\sim 23 \text{ nm}$ for undoped and Eu^{3+} doped La_2O_3 respectively.

3.2. Thermoluminescence

Fig. 2 shows TL glow curve of La_2O_3 samples irradiated with γ -rays (^{60}Co) with energy 1.2 MeV for different exposures in the range 0.05–12.0 kGy recorded at a heating rate of 5 K s^{-1} . Undoped sample shows two TL glows with high intense peak at 640 K and weak one with a peak at 443 K. These TL glows are attributed to the presence of oxygen vacancies in the sample [12,13]. Fig. 3 shows TL glow peak (640 K) intensity and glow peak temperature as a function of γ -irradiation dose. It is observed that the glow peak

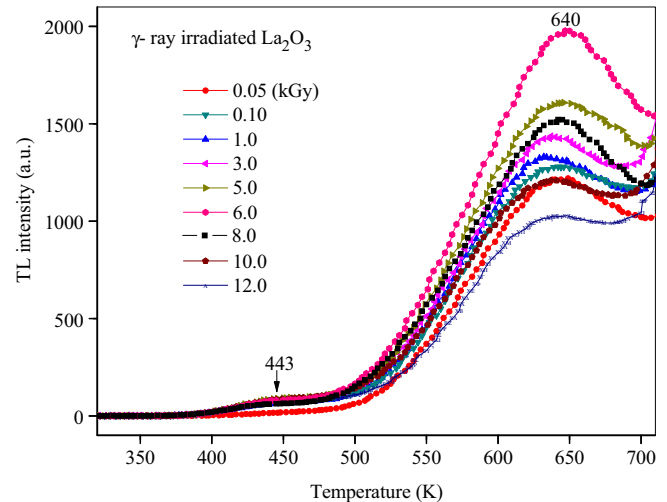


Fig. 2. TL glow curves of γ -ray irradiated La_2O_3 nanoparticles.

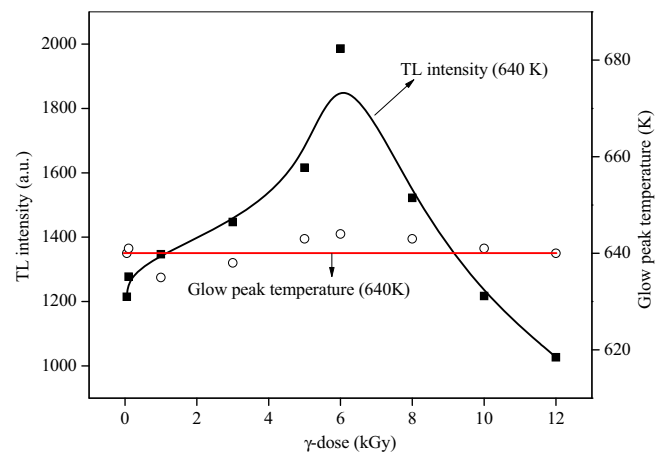


Fig. 3. Variation of TL glow peak intensity and glow peak temperature with γ -dose for undoped La_2O_3 nanoparticles.

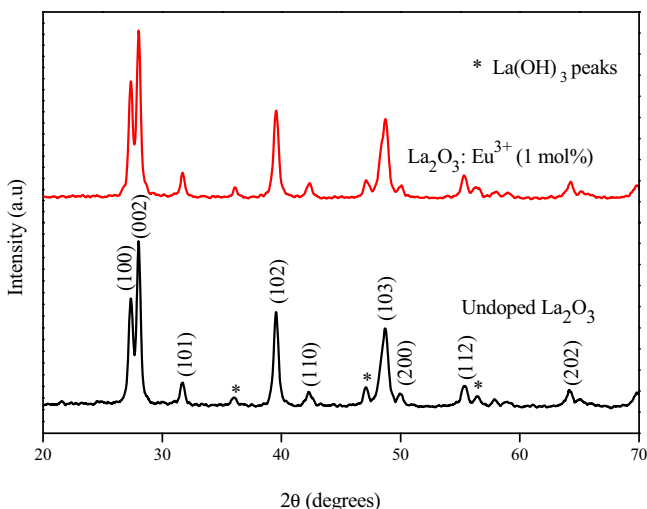


Fig. 1. X-ray diffraction pattern of undoped and Eu^{3+} (1 mol%) doped La_2O_3 nanoparticles.

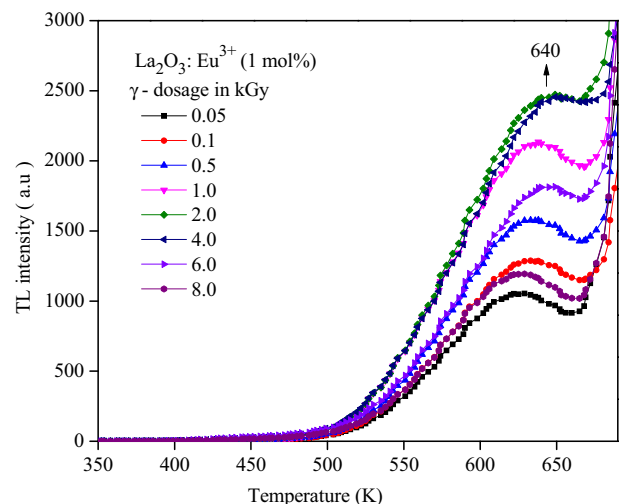


Fig. 4. TL glow curves of γ -ray irradiated $\text{La}_2\text{O}_3:\text{Eu}^{3+}$ (1 mol%) nanoparticles.

(640 K) intensity sub-linearly increases with increase in γ -ray dose up to 6 kGy and thereafter decreases. Further TL properties Eu^{3+} -doped lanthanum oxide is studied to improve the TL response.

Fig. 4 shows TL glow curve of $\text{La}_2\text{O}_3:\text{Eu}^{3+}$ (1.0 mol%) samples irradiated with γ -rays in the dose range 0.05–8.0 kGy at room temperature. A broad high temperature TL glow with peak at 640 K is observed for all doses, but the low temperature glow peak is disappeared after Eu^{3+} doping. It might be attributed to Eu^{3+} ions occupied in La^{3+} sites, it is modified the crystal symmetry of La_2O_3 lattice and band gap of the material. Fig. 5 shows the TL glow peak (640 K) intensity and glow peak temperature as a function of γ -irradiation dose. It is observed that the glow peak intensity linearly increases with increase of γ -dose from 0.05 to 1.0 kGy and then sub-linearly increased up to 2.0 kGy, thereafter decreases with further increase of γ -doses. But glow peak temperature changed within experimental error (± 5 K). The increase in TL intensity might be attributed to the creation of defect centers such as F and F^+ centers. Decrease in TL intensity with increase of γ -dose may be attributed to the formation of F-aggregated center [14]. This can be explained by the defect interaction model [14]. According to this, recombination within the trapping center/luminescence center (TC/LC) dominates at the lower doses, leads to a linear response. Increase in TL intensity with dose indicates that more and more number of electrons and hole traps are created and those electrons recombine with holes at the luminescence center giving raise to TL signal. Further increases in γ -dose, the separation between adjacent TC/LC are reduced, which results in formation of cluster defects, leads to decrease in TL signal [14].

3.2.1. Kinetic parameters

To understand the TL properties of the material requires detailed knowledge of kinetic parameters such as activation energy (E) of the traps involved in TL, order of kinetics (b) and frequency factor (s) associated with the glow peaks of TL. Here, E is the energy required to release of charge carrier from the trap to reach its excited state and 's' is the rate of electron ejection. The order of kinetics 'b' is the measure of the probability that a free electron gets retrapped or recombine with holes. To obtain these parameters, the glow curves are deconvoluted using a glow curve deconvolution (GCD) technique [15]. The detail GCD technique is discussed by Kitis et al. [16]. The deconvoluted TL curve of La_2O_3 irradiated with γ dose of 6 kGy is shown in Fig. 6. It is observed the glow curve is deconvoluted into four peaks at 442, 525, 595 and 663 K and $\text{La}_2\text{O}_3:\text{Eu}^{3+}$ phosphor (Fig. 7) is deconvoluted into two peaks at 583 K and 640 K. The theoretically fitted TL glow

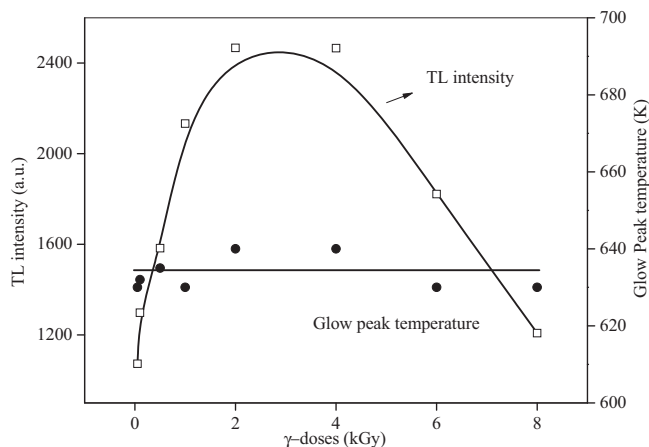


Fig. 5. Variation of TL glow peak intensity and glow peak temperature with γ -doses for $\text{La}_2\text{O}_3:\text{Eu}^{3+}$ (1 mol%) nanoparticles.

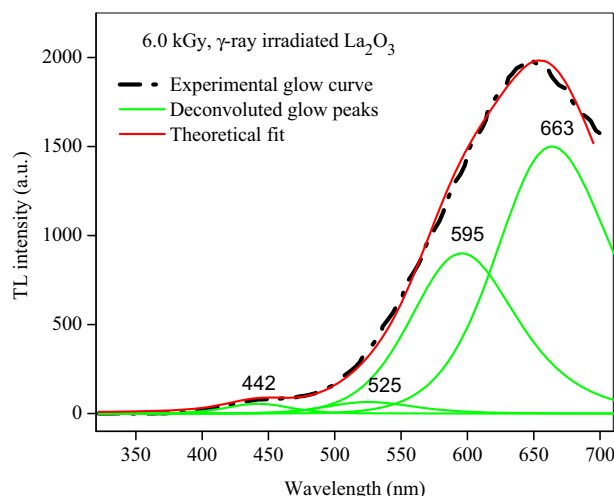


Fig. 6. TL deconvoluted glow curves of 6 kGy γ -ray irradiated La_2O_3 nano phosphor.

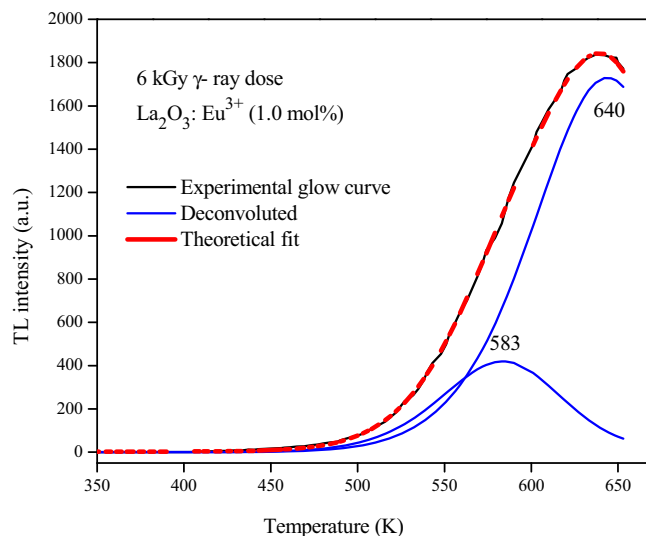


Fig. 7. TL deconvoluted glow curves of 6 kGy γ -ray irradiated $\text{La}_2\text{O}_3:\text{Eu}^{3+}$ nanophosphor.

curves are well fitted with the experimental data and the quality of fitting is described by figure of merit (FOM) [17]. The FOM for the present curve fitting is 1.82 and 2.2% for undoped and Eu^{3+} doped La_2O_3 , respectively. Which indicates that a good agreement between theoretically fitted and experimentally recorded TL glow curves. The trap parameters of TL curves are calculated using the curve fitting method [15]. The obtained TL kinetics parameters are tabulated in Table 1. It shows that the order of kinetics (b) of low temperature glow peaks obeys general order due to equal probability of recombination and retrapping centers and high

Table 1
TL kinetic parameters of undoped and $\text{La}_2\text{O}_3:\text{Eu}^{3+}$ (1 mol%) nanoparticles.

Sample (6.0 kGy)	T_m (K)	b	Activation energy (eV)	Frequency factor (s^{-1})
Undoped La_2O_3	442	1.7	0.9	4.62×10^9
	525	2.0	1.0	7.68×10^8
	595	2.0	1.1	1.22×10^8
	663	2.0	1.2	1.91×10^8
Eu^{3+} doped La_2O_3	583	1.5	1.0	7.18×10^7
	640	2.0	1.1	5.87×10^7

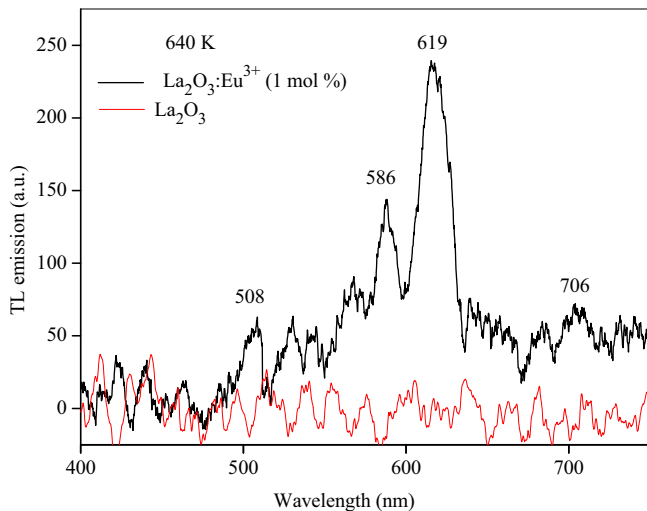


Fig. 8. TL emission of γ -ray irradiated $\text{La}_2\text{O}_3:\text{Eu}^{3+}$ nanophosphor.

temperature glow peaks obeys second order kinetics due to re-trapping is more. It is observed that activation energies are increased and frequency factors are decreased with increasing TL glow peak temperature. It indicates that the traps are located in deeper traps level in the band gap of the material. Fig. 8 show a typical TL emission spectrum of 2 kGy γ -ray irradiated undoped and $\text{La}_2\text{O}_3:\text{Eu}^{3+}$ nanophosphor. The undoped sample do not shows emission in recorded temperature range (325–750 K) but Eu^{3+} doped phosphor shows maximum TL emission intensity with peaks at 508, 586, 619 and 706 nm at 640 K and corresponding peaks are attributed to Eu^{3+} transitions.

4. Conclusion

Undoped and Eu^{3+} doped La_2O_3 nanophosphor are synthesized by the sol-gel technique at low temperature. The synthesized sample shows hexagonal phase upon annealed at 800 °C. Gamma irradiated undoped and Eu^{3+} doped La_2O_3 nanophosphor shows a

prominent TL glow peak at 640 K. TL response of undoped sample exhibit sublinearity with dose, whereas Eu^{3+} doped La_2O_3 nanophosphor shows linear response up to 1 kGy, since a linear variation of TL intensity is one of the important characteristics of TL dosimeter. Hence Eu^{3+} doped La_2O_3 nanophosphor might be suitable for an high energy dosimetry application.

Acknowledgment

The Authors (P.N. & M.K.K.) acknowledge Department of Atomic Energy and Board of Research in Nuclear Science (DAE-BRNS), BARC, India for providing financial support (project No.2011/37P/18/BRNS).

References

- [1] Z. Xu, S. Bian, J. Wang, T. Liu, L. Wang, et al., *RSC Adv.* (2013) 1410–1419.
- [2] M. Chandrasekhar, D.V. Sunitha, N. Dhananjaya, H. Nagabhushana, S.C. Sharma, B.M. Nagabhushana, *Mater. Res. Bull.* 47 (2012) 2085–2094.
- [3] H. Huang, H. Zhang, W. Zhang, S. Lian, Z. Kang, Y. Liu, *J. Lumin.* 132 (2012) 2155–2160.
- [4] Wu, Chia-Song, Liu, Hsing-Chung, *J. Semicond.* 30 (2009) 114004-1–114004-4.
- [5] G. Li, M. Shang, D. Geng, D. Yang, C. Peng, J. Lin, *Cryst. Eng. Comm.* (2012) 2100–2111.
- [6] N. Salah, P.D. Sahare, *J. Phys. D: Appl. Phys.* 39 (2006) 2684–2691.
- [7] S.W.S. Mckeever, *Thermoluminescence of Solids*, Cambridge University Press, 1985.
- [8] S.P. Lochab, D. Kanjilal, N. Salah, S.S. Habib, Jyoti Lochab, R. Ranjan, V.E. Aloychnikov, A.A. Rupasov, A. Pandey, *J. Appl. Phys.* 104 (2008) 033520–033523.
- [9] Yury. Gogotsi, *Nanomaterials Hand Book* CRC Press, Taylor & Francis, New York, 2006.
- [10] B.N. Lakshminarasappa, N.J. Shivaramu, K.R. Nagabhushana, Fouran Singh, *Nucl. Inst. Methods Phys. Res.* 329 (2014) 40–47.
- [11] M. Back, A. Massari, M. Boffelli, F. Gonella, P. Riello, D. Cristofori, R. Ricco, F. Enrichi, *J. Nanopart. Res.* 14 (2012) 792.
- [12] B.C. Hu, H. Liu, W. Dong, Y. Zhang, G. Bao, C. Lao, *Adv. Mater.* (2007) 470–474.
- [13] N.J. Shivaramu, B.N. Lakshminarasappa, K.R. Nagabhushana, F. Singh, *Radiat. Meas.* 71 (2014) 518–523.
- [14] S. Mahajna, Y.S. Horowitz, *J. Phys. D: Appl. Phys.* 30 (1997) 2603–2619.
- [15] D. Afouxenidis, G.S. Polymeris, N.C. Tsirliganis, G. Kiti, *Radiat. Prot. Dosim.* 149 (2012) 363–370.
- [16] G. Kitis, J.M. Gomez Ros, J.W.N. Tuyn, *J. Phys. D: Appl. Phys.* 31 (1998) 2636–2641.
- [17] N. Kaur, L. Singh, M. Singh, S.P. Lochab, *Nucl. Instr. Methods Phys. Res. Sect. B Beam Interact. Mater. Atoms* 290 (2012) 1–5.